

Observation of molecular layering in a confined water film and study of the layers viscoelastic properties

M. Antognozzi,^{a)} A. D. L. Humphris, and M. J. Miles

University of Bristol, H. H. Wills Physics Laboratory, Tyndall Avenue, Bristol BS8 1TL, United Kingdom

(Received 7 August 2000; accepted for publication 15 November 2000)

A transverse dynamic force microscope, more commonly known as shear force microscope, has been used to investigate confined water films under shear. A cylindrically tapered glass probe was mounted perpendicularly to the sample surface. Pure water was confined between the probe and a freshly cleaved mica surface and a sinusoidal shear strain was applied by setting the probe into transverse oscillation. Repeated measurements of the probe oscillation amplitude and relative phase lag, at different tip-sample separations, exhibited a clear step-like behavior. The periodicity, recorded over several curves, ranged between 2.4 and 2.9 Å, which is similar to the diameter of the water molecule. The in-phase (elastic) and the out-of-phase (viscous) stress response of the confined water film was evaluated (from the experimental data) by assuming a linear viscoelastic behavior. Finally, by modeling the water film with the Maxwell mechanical model, the values for the shear viscosity and shear rigidity were obtained. © 2001 American Institute of Physics.
[DOI: 10.1063/1.1339997]

With the development of the surface force apparatus (SFA)¹ and atomic force microscopy (AFM)² it has become possible to study the behavior of confined liquid films only a few nanometers thick. The importance of these investigations is easy to understand considering the large number of related applications, ranging from lubrication, friction, and adhesion to biological membranes.

When liquid molecules are confined between two smooth hard surfaces they are organized in discrete layers.³ The reason for this behavior is, in part, due to the geometry of the system (this is why the same effect is present in non-interacting molecules and surfaces) and in part to the interaction energy between the walls and the solvent molecules.

Associated with the layer structure of the density profiles is the presence of oscillatory solvation forces between the surfaces. Experimental and theoretical work has demonstrated the oscillatory nature of these interactions with a period comparable to the molecular diameter. In order to see the oscillatory behavior, the confining walls have to be molecularly smooth and, if the surfaces are monocrystalline, they may induce a further organization in the plane of the layers (as molecular dynamics simulations⁴ and scanning tunneling microscopy^{5,6} have shown for adsorbed water).

When a fluid is highly confined an increase in its effective viscosity and the manifestation of an elastic behavior are produced. These two effects are more characteristic of a “solid-like” structure than of a fluid. For this reason, in the last years, several studies have been dedicated to these systems⁷⁻⁹ and especially to identifying possible phase transitions induced by confinement.¹⁰⁻¹⁵

In this letter the possibility of using transverse dynamic force microscopy (TDFM), more commonly known as shear force microscopy, in the study of confined liquids under shear is presented. This scanning probe microscope is, in

fact, particularly well suited for dynamic measurements of viscoelastic properties, as will be shown later.

In TDFM a tapered optical fiber is mounted vertically and perpendicularly to the sample surface and set in horizontal oscillation using a dither piezo. The oscillation amplitude and the corresponding phase signal are quantitatively measured with an optical detection system.¹⁶ The tapered probe is obtained by pulling and fracturing an optical fiber heated in the beam of a CO₂ laser.¹⁷ This technique produces a flat circular end with ~50 nm radius (as scanning electron microscopy pictures have revealed).

When the vibrating probe is brought within a few nanometers of the sample surface, capillary condensation takes place and a water bridge is formed.^{18,19} The condensation is due to the water present on both the probe and the sample and on the ambient relative humidity.³ If a drop of distilled water is deposited on the sample surface then it is no longer necessary to rely on the capillary condensation and the results in both cases are essentially the same. The only difference is the higher hydrodynamic damping experienced by the probe in the second case.

In TDFM, a known sinusoidal shear strain is imposed on the confined fluid and the corresponding stress response is evaluated. Figure 1 shows all the important elements involved in a typical force spectroscopy experiment. A sinusoidal displacement ($d_0 \sin \omega t$) is applied at the top end of the probe. The corresponding oscillation amplitude and phase [$u_0 \sin(\omega t + \phi)$] are recorded at the lower end. This point is where the force, due to the shear stress response of the fluid, is operating. Shear strain and the shear stress can be derived from displacement/(tip-sample separation) and force/(tip area), respectively.

If the confined liquid acts as a linear viscoelastic material then the resulting stress has an in-phase and an out-of-phase component with respect to the strain.²⁰ Assuming a sinusoidally varying strain

^{a)}Electronic mail: m.antognozzi@bristol.ac.uk

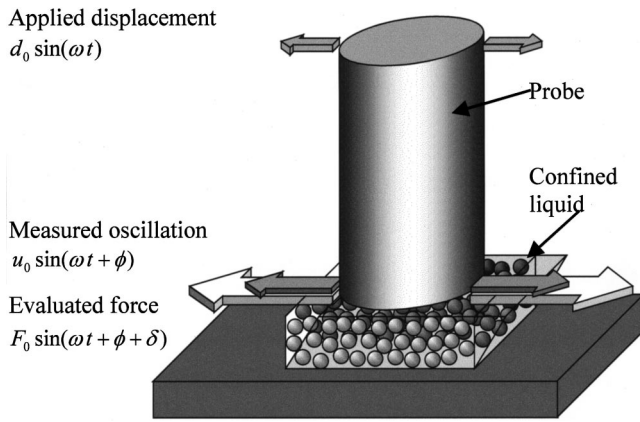


FIG. 1. Model for the TDFM used for dynamic (oscillatory) measurements of stress response to an applied strain. The viscoelastic behavior of the confined fluid results in a phase difference δ between the stress and strain. Measuring the change (with respect to the free vibration) in the oscillation amplitude u_0 and in the phase ϕ it is possible to calculate the in-phase and out-of-phase components of the interacting force.

$$\gamma = \gamma_0 \sin \omega t; \quad (1)$$

the stress response is determined by the following constitutive equation:

$$\sigma = \gamma_0 (G' \sin \omega t + G'' \cos \omega t), \quad (2)$$

where G' is the shear storage modulus and G'' is the shear loss modulus. The phase lag δ between stress and strain is given by

$$\tan \delta = G''/G'. \quad (3)$$

The change in the dynamic properties of the probe (amplitude and phase) is the key to calculating the stress response. As already described by Kirsh *et al.*,²¹ the harmonic oscillator model can be used to evaluate, from this amplitude and phase values, the damping coefficient and the resonant frequency of the probe. These two parameters are related to the viscous and elastic shear force of the tip-liquid interaction. Unfortunately it is difficult, without some assumptions (for example the effective mass of the probe), to extract quantitative information from this model. In the present work, the dynamics of the probe have been modeled using continuum mechanics (solving the Euler–Bernoulli beam equations). Discrete element analysis has also been implemented in order to take into account the tapered region of the probe.²² The probe is divided into a number of sections, n , perpendicularly to the longitudinal axis and of suitable radius r . Each section is described by the Euler–Bernoulli equation

$$E(1 + i\alpha)I_j \frac{\partial^4 Y}{\partial \zeta^4} + 2\gamma_j r_j \frac{\partial Y}{\partial t} + A_j \sigma \frac{\partial^2 Y}{\partial t^2} = 0, \quad (4)$$

where the subscript j refers to the particular section considered. $Y(\zeta, t)$ describes the shape of the vibrating probe as a function of the position along the probe axis ζ and of the time t . The Young's modulus E of the probe is written in complex notation to take into account the internal friction, and α is usually defined as the *loss modulus*.²³ The second term in Eq. (4) describes the interaction with the surrounding medium for the considered section. γ_j represents the viscous coefficient of the water (air) if the section is below (above) the water level. A_j and σ are the cross-sectional area and the

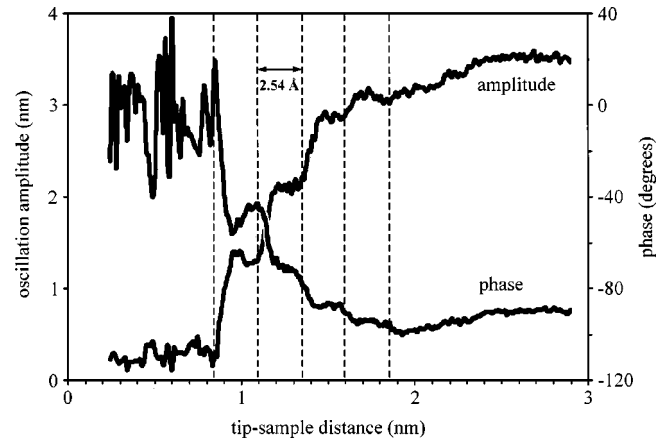


FIG. 2. Amplitude and phase approach curves acquired in pure water over a freshly cleaved mica surface. The steps revealed in the curves are due to the molecular layering of water in the confined space between the probe and the mica surface. The four equispaced vertical lines have been drawn to emphasize the periodicity.

density, respectively. Continuity of the solution and equilibrium of the total bending moment and shear force between the sections is ensured by matching the boundary conditions at each of the $(n-1)$ interfaces. Two additional conditions are imposed at each of the two extremities of the probe. The shear force interaction between the flat end of the probe and the sample is introduced as one of these conditions.

In Fig. 2, the oscillation amplitude and the phase lag are shown as the tip approaches a freshly cleaved mica surface. The curves were obtained in pure water (18 M Ω Elgar Stat) as described earlier. The approach speed was 10 nm/s and the shear frequency (i.e., the resonant frequency of the probe) was 10.5 kHz. Similar results were obtained for different approach speeds (between 2 and 10 nm/s) and shear rates (between 1 and 20 kHz). An estimation of the point of contact is obtained by monitoring the dc signal from the two-sector photodiode. A sudden discontinuity is, in fact, measured when the probe makes contact with the surface. The results shown in Fig. 2 also confirm tunneling current measurements obtained simultaneously to oscillation amplitude measurements. In this case a conductive tungsten probe was approaching a graphite surface in ambient conditions. It was found that, when the oscillation amplitude vanished, the probe was still around one nanometer far from the tunneling regime.²⁴

The curves in Fig. 2 clearly present four steps in both amplitude and phase. The mean periodicity for this particular set of data is 2.54 Å but repeated measurements gave values ranging between 2.4 and 2.9 Å. These results are in very good agreement with the periodicity of 2.5 ± 0.3 Å reported by Israelachvili⁸ from SFA measurements. Figure 3 shows the elastic (in-phase) and viscous (out-of-phase) forces calculated from the constitutive Eq. (2) assuming a tip area of 7.8×10^{-3} nm². As already pointed out by other authors,²⁵ it is difficult to establish a standard technique for shear measurements of confined liquids. Nevertheless some important characteristics of the TDFM results can be grasped by analyzing the two force curves in Fig. 3.

(1) The dissipative component dominates for tip-sample separations greater than 1.6 nm but becomes less significant

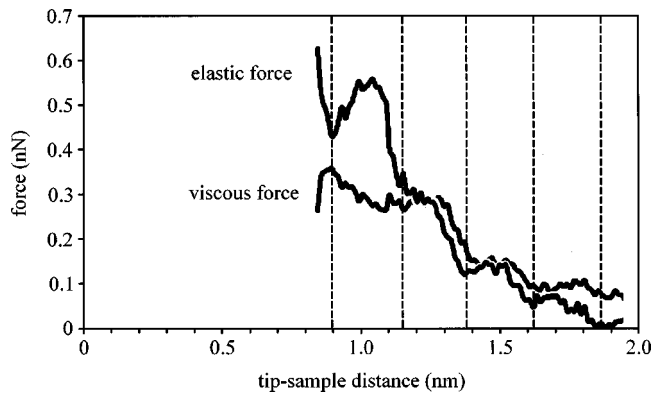


FIG. 3. Evaluated forces (viscous and elastic) from the approach curves shown in Fig. 1. The dissipative viscous force dominates over the elastic component at the start of the interaction but becomes less significant when the tip-sample distance is less than 1.5 nm.

closer to the surface. The elastic force, on the other hand, increases rapidly with the decreasing separation.

(2) Fine structure within each step can be observed. For the initial two steps both the forces have a similar behavior. They remain constant before sharply increasing. On the other hand, the last two steps exhibit almost the inverse situation between the two forces. When one curve rises the other diminishes and vice versa. This result shows that a different viscoelastic behavior of the confined fluid pertains inside each molecular layer. Furthermore, this behavior is also dependent on the number of water layers, between the glass tip and the mica surface.

(3) For separations smaller than four molecular layers the drive frequency is outside the bandwidth of the frequency response of the probe due to the shift in its resonant frequency. As a consequence, the signal-to-noise ratio is significantly reduced.

By using the Maxwell mechanical model of a viscoelastic material (a dashpot in series with a spring) a simple description of the confined liquid can be attempted. This model is usually applied to “liquid-like” bodies which cannot sustain stress.²⁰ The shear rigidity k is associated with the spring and the viscosity η is associated with the dashpot. The relationships between these two parameters and the two moduli G' and G'' are given later.

$$G' = k\omega^2\eta^2/(k^2 + \omega^2\eta^2), \quad (5)$$

$$G'' = k^2\omega\eta/(k^2 + \omega^2\eta^2). \quad (6)$$

The relaxation time τ is defined as η/k . This quantity is important as it can be used to discriminate between “solid-like” and liquid-like behavior.²⁵ In Fig. 4, the shear rigidity, the shear viscosity and the relaxation time, are deduced from the curves in Fig. 3.

In conclusion, the shear force microscope has been shown to resolve the layered structure of confined water under shear and the interlayer spacing obtained with this technique are consistent with the results obtained via SFA.⁸

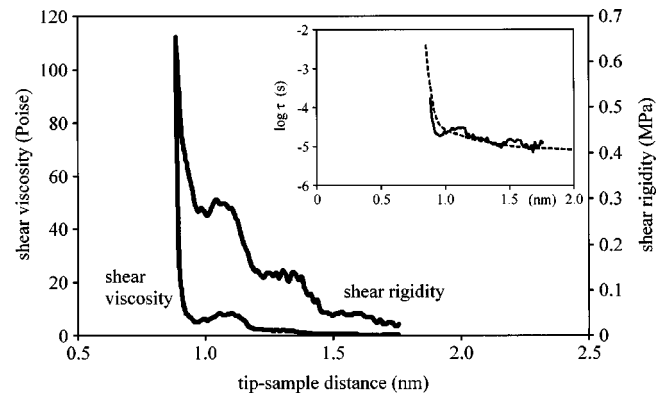


FIG. 4. Shear rigidity k and viscosity η evaluated from the force curves (shown in Fig. 3) assuming a tip radius of 50 nm. These high values (if compared with values for bulk distilled water) can be explained by the increasing confinement of the water between the tip and the mica surface. In the inset the relaxation time τ has been calculated (the dot line has been drawn to guide the eyes.)

These results are possible owing to the geometry of the microscope that offers true tip-sample distance control whereas SFA and AFM both suffer from instability in distance control. By modeling the tip-sample interaction as a viscoelastic force it has been possible to describe separately the elastic and viscous forces within the observed layer structure. Furthermore, the use of the Maxwell model of viscoelastic fluids allowed us to estimate shear viscosity and shear rigidity of the confined water film.

- ¹J. N. Israelachvili and G. E. Adams, *J. Chem. Soc., Faraday Trans. 1* **74**, 975 (1978).
- ²G. Binnig, C. F. Quate, and Ch. Gerber, *Phys. Rev. Lett.* **56**, 930 (1986).
- ³J. N. Israelachvili, *Intermolecular and Surface Forces* (Academic, London, 1985), Chap. 13.
- ⁴W. Ranke, D. Schmeisser, and Y. R. Xing, *Surf. Sci.* **152/153**, 1103 (1985).
- ⁵M. Morgestern, J. Müller, T. Michely, and G. Comsa, *Z. Phys. Chem. (Munich)* **198**, 43 (1997).
- ⁶A. Marmier, P. N. M. Hoang, S. Picaud, C. Girardet, and R. M. Lynden-Bell, *J. Chem. Phys.* **109**, 3245 (1998).
- ⁷R. G. Horn and J. N. Israelachvili, *J. Chem. Phys.* **75**, 1400 (1981).
- ⁸J. N. Israelachvili and R. M. Pashley, *Nature (London)* **306**, 249 (1983).
- ⁹D. L. Patrick and R. M. Lynden-Bell, *Surf. Sci.* **380**, 224 (1997).
- ¹⁰S. Granick, *Science* **253**, 1374 (1991).
- ¹¹J. Klein and E. Kumacheva, *J. Chem. Phys.* **108**, 6996 (1996).
- ¹²J. Gao, W. D. Luedtke, and U. Landman, *J. Chem. Phys.* **106**, 4309 (1997).
- ¹³M. Shoen and H. Bock, *J. Phys.: Condens. Matter* **12**, A333 (2000).
- ¹⁴H. Domingez, M. P. Allen, and R. Evans, *Mol. Phys.* **96**, 209 (1999).
- ¹⁵M. Sliwinska-Bartkowiak, J. Gras, R. Sikorski, R. Radhakrishnan, L. Gelb, and K. E. Gubbins, *Langmuir* **15**, 6060 (1999).
- ¹⁶M. Antognozzi, H. Haschke, and M. Miles, *Rev. Sci. Instrum.* **71**, 1689 (2000).
- ¹⁷R. L. Williamson and M. J. Miles, *J. Appl. Phys.* **80**, 4804 (1996).
- ¹⁸S. Davy, M. Spajer, and D. Courjon, *Appl. Phys. Lett.* **73**, 2594 (1998).
- ¹⁹R. Brunner, O. Marti, and O. Hollricher, *J. Appl. Phys.* **86**, 7100 (1999).
- ²⁰J. D. Ferry, *Viscoelastic Properties of Polymers* (Wiley, New York, 1970).
- ²¹A. K. Kirsch, C. K. Meyer, and T. M. Jovin, *J. Microsc.* **185**, 396 (1997).
- ²²M. Antognozzi, D. R. Binger, A. D. L. Humphris, P. J. James, and M. J. Miles, *Ultramicroscopy* (to be published).
- ²³N. O. Myklestad, *J. Appl. Mech.* **19**, 284 (1952).
- ²⁴L. Brereton, Ph.D. thesis, Bristol, 1998.
- ²⁵A. L. Demirel and S. Granick, *Phys. Rev. Lett.* **77**, 2261 (1996).